

# Lawrence Berkeley National Laboratory

## LBL Publications

### Title

Optimization studies on high-strength Ag-Cu conductors

### Permalink

<https://escholarship.org/uc/item/52h598v4>

### Authors

Heringhaus, F  
Prestemon, SO  
Gottstein, G  
et al.

### Publication Date

1998

Peer reviewed

## OPTIMIZATION STUDIES ON HIGH-STRENGTH Ag -Cu CONDUCTORS

F. Heringhaus,<sup>1,2</sup> S.O. Prestemon,<sup>1</sup>  
G. Gottstein,<sup>2</sup> and H.-J. Schneider-Muntau<sup>1</sup>

<sup>1</sup> National High Magnetic Field Laboratory, Tallahassee, Florida, USA  
1800 East Paul Dirac Drive, Tallahassee, Florida, 32306-4005, USA

<sup>2</sup> Institut für Metallkunde und Metallphysik, RWTH Aachen, Germany  
Kopernikusstraße 14, Aachen, 52074, Germany

### ABSTRACT

Changes in the microstructure of a material can strongly influence the macroscopic material properties. A careful study of the properties as a function of the microstructure, varied as a response to deformation for example, can allow for an optimization of the material for a combination of properties.

Such an optimization study is demonstrated here for the example of a lamellar eutectic material, Ag-Cu, the microstructure of which has been investigated by quantitative transmission electron microscopy at various degrees of plastic deformation. The properties investigated are mechanical strength, electrical resistivity, and thermal resistivity. The experiments have been carried out at room temperature and cryogenic temperatures (77 and 4.2 K).

Through correlation of each of these properties with the microstructure development, an optimum microstructure can be determined for a given combination of properties at a specified temperature of operation.

The motivation for this study is the optimization of high strength conductors as used in high field magnets. The combination of high strength and high conductivity in these conductors allows for the design of high-field magnets with pulsed fields up to 75 tesla and steady-state fields of 33 tesla.

### INTRODUCTION

During the operation of high-field magnets, mechanical forces are exerted on the conductor itself and electrical energy is converted into heat. Either one or a combination

of both in excess of the material's and magnet design limits can lead to magnet failure. To withstand the stresses and to minimize heating, materials are needed that combine both high mechanical strength and high electrical conductivity.

For this application both macrocomposite and microcomposite materials are being used. Since macrocomposites commonly follow the rule of mixtures (ROM), their properties change linearly between their constituent properties and thus depend solely on their volumetric fraction. This, however, does not hold for microcomposites such as Cu-18wt.%Nb<sup>1,2</sup> and Cu-24wt.%Ag<sup>3,4</sup>, which are the prototypes of such high strength microcomposite conductors. The fineness of the microstructure and the amount of internal interface lead to deviations from the ROM. Since the various properties of microcomposites respond differently to changes in the microstructure, their ratio varies not only non-linearly with composition but also with the microstructure itself.

The microcomposite Cu-24wt.%Ag consists of two microstructure constituents, the primary  $\alpha_{Cu}$  with a maximum solubility for Ag of 7.9wt.% at 1054K and eutectic Ag-Cu at 28.1wt.% (31.5vol.%) Cu<sup>5</sup>. The former can be heat treated for precipitation strengthening in conjunction with matrix purification for increased conductivity<sup>6</sup>. The latter solidifies in lamellar or rod form depending on homogeneity and cooling conditions<sup>7-9</sup>. In this study, we regard the eutectic only.

Material of eutectic composition was chill cast and plastically strained by rotary swaging from 25 to 0.53 mm and a total logarithmic deformation of  $\eta=7.72$ . The microstructure was quantified by scanning (SEM) and transmission (TEM) electron microscopy. Properties of interest to application in high field magnets were investigated at 295, 77, and 4.2 K.

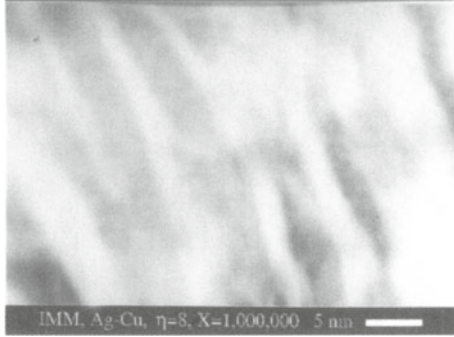
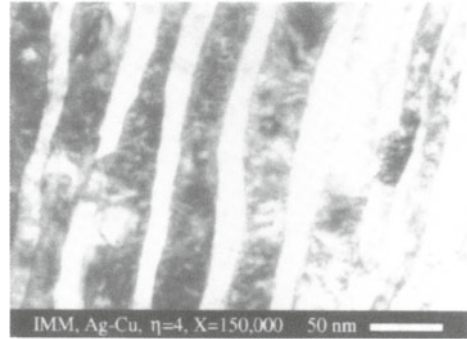
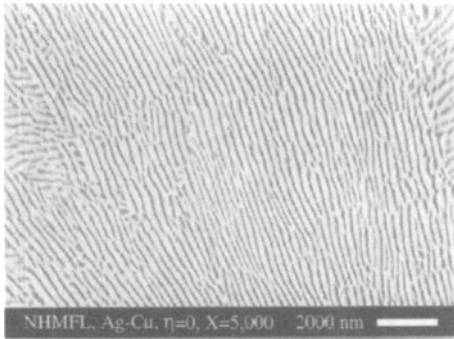
The purpose of this study is to find the optimum microstructure of eutectic Ag-Cu for a combination of high mechanical strength and high electrical conductivity. Furthermore, we want to present an approach to determine the optimum microstructure for any given combination of properties.

## MICROSTRUCTURE

A typical SEM micrograph of the as-cast state of Ag-Cu is given in Figure 1. The light phase is Ag-rich, the dark phase is Cu-rich. The phase arrangement is strongly lamellar, however, few (<1vol.%) rod shape eutectic regions of Cu in a Ag matrix have been observed. Regions between eutectic grains are commonly found to be Ag rich. No preferred topological orientation of the lamellae axes with respect to the orientation of the cast rod was observed.

Plastic deformation of the composite leads to a decrease in the average lamellae thickness of both phases, as is shown in the TEM micrographs in Figures 2 and 3. Note that the contrast of the phases Ag and Cu in the TEM micrographs is typically reversed with respect to the SEM micrographs. The average lamellae thicknesses of the Ag and Cu phases, respectively, reduce from approximately 240 and 100 nm for the as-cast state (Figure 1) to 35 and 18 nm at  $\eta=4$  (Figure 2), and 4.6 and 2.6 nm at  $\eta=7.72$  (Figure 3).

A quantitative analysis of the microstructure is presented in Figure 4 for the Ag and the Cu phase in Ag-Cu. For both phases, an exponential decrease of the average lamellae thickness with the wire deformation was found. In the as-cast state, the standard deviation from the average was around 30%. With ongoing deformation, the standard deviation decreases to below 10%. The decrease in the thickness of the Ag lamellae is stronger (exponent = -0.5127  $\eta$ ) than the decrease in the thicknesses of the Cu lamellae



Micrographs of eutectic Ag-Cu.

**Figure 1 (top left).** SEM micrograph,  $\eta=0$ , as-cast, Ag phase: light, Cu phase: dark.

**Figure 2 (top right).** TEM micrograph,  $\eta=4.03$ ,  $\epsilon=98.20\%$ , Cu phase: light, Ag phase: dark.

**Figure 3 (left).** TEM micrograph,  $\eta=7.72$ ,  $\epsilon=99.96\%$ , Cu phase: light, Ag phase: dark.

(exponent =  $-0.4799 \eta$ ). Averaging the reduction in lamellae thicknesses, with respect to the volume fraction of the phases, leads to an exponent of  $-0.5066 \eta$ , describing the reduction from approximately 200 nm in the as-cast state to 4 nm at  $\eta=7.72$ .

## PROPERTIES

The macroscopic properties of Ag-Cu can be subdivided into two groups: those that are independent of the microstructure and hence follow the predictions of the ROM, and those that depend on the microstructure.

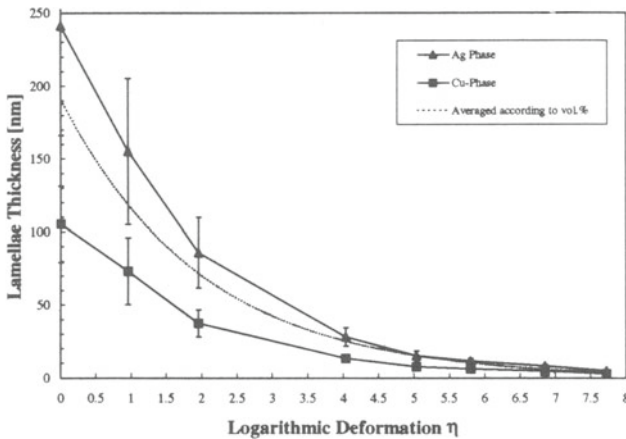


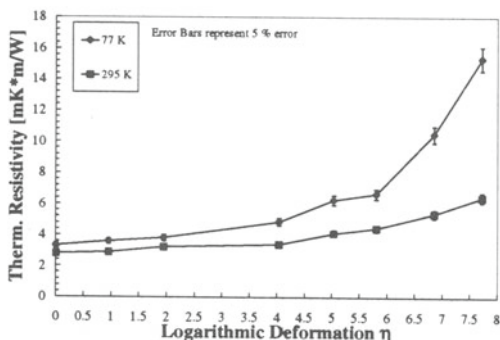
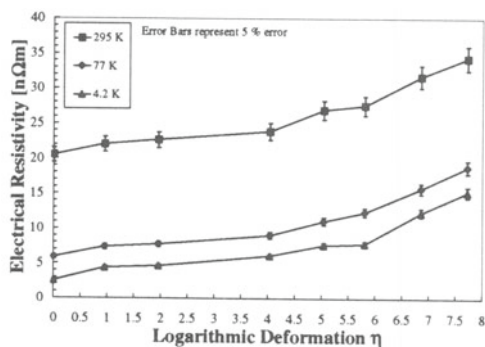
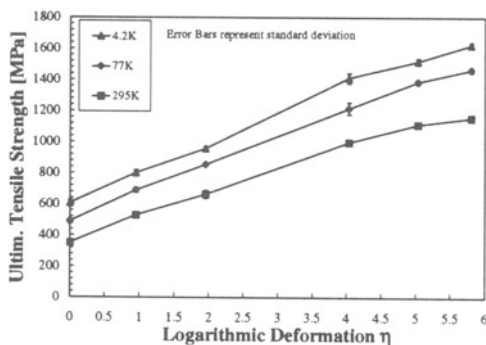
**Figure 4.** Lamellae thicknesses of the Ag and Cu phases as a function of the wire deformation. The dotted line represents the lamellae thickness averaged according to the volume fraction of the phases.

To the extent that the microstructure was varied in this study, only two of the investigated properties have been found not to depend on the microstructure, namely the magnetic susceptibility and the specific heat. Figures 5 - 7 show the development of the ultimate tensile strength (UTS), the electrical resistivity, and the thermal resistivity of Ag-Cu as a function of the wire deformation for three temperatures. The differences between ROM values and experimental findings after the highest degree of deformation ( $\eta=7.72$ ) amount to about 200% for the UTS (Figure 5) at all three temperatures. The electrical resistivity (Figure 6) reveals a 73, 216, and 344 % change at 295, 77, and 4.2 K, respectively and the thermal resistivity (Figure 7) changes of 167% at 295K and 658% at 77K.

## MATERIALS OPTIMIZATION

Since the changes of the macroscopic properties as a function of the microstructure development depend on the investigated property, an optimization is possible that allows for the determination of the microstructure that yield certain combinations of properties. This is demonstrated for a combination of UTS and electrical resistivity first, followed by a description on how to apply this model to a larger set of properties. An application to a combination of three properties is carried out and presented.

Figure 8 demonstrates that the UTS and the electrical resistivity, normalized to their respective ROM values, have different slopes when depicted as a function of the lamella thickness. An optimum combination of the two properties is achieved at a lamella thickness where the ratio of their slopes,  $k$ , in Eq. (1) is unity. At a lamella thickness with  $k > 1$ , each incremental decrease in lamella thickness leads to an increase in strength that is larger than the increase in resistivity. At a lamellae thickness with  $k < 1$ , each incremental increase in lamella thickness leads to a decrease in resistivity that exceeds the decrease in strength.



Properties of eutectic Ag-Cu as a function of the wire deformation.

**Figure 5 (top left).** Ultimate tensile strength (UTS) at 295, 77, and 4.2 K.

**Figure 6 (top right).** Electrical resistivity at 295, 77, and 4.2 K.

**Figure 7 (left).** Thermal resistivity at 295 and 77 K.

$$\frac{\left[ d \left( \frac{UTS}{UTS_{ROM}} \right) \right]}{\left[ d \left( \frac{\rho}{\rho_{ROM}} \right) \right]} = k_{UTS,\rho} \quad (1)$$

Certain applications, however, may not call for the optimum combination of two properties,  $P_i$  and  $P_j$ , but for a defined preference of one, e.g., higher strength for inner magnet coils that operate in a high background field, or lower electrical resistivity for outer magnet coils that carry high currents. This preference can be accounted for by changing the derivative ratio,  $k_{ij}$ , and solving Eq. (2) with respect to the lamella thickness. Note that  $\tilde{P}$  represents the property,  $P$ , normalized to its respective ROM value. This is demonstrated in Figure 9 for combinations of UTS and electrical resistivity at 77 K. For preferences of derivative ratios,  $k$ , between 0.3 and 1.7, the optimum lamella thickness varies between 3 and 29 nm.

Due to the temperature dependence of the slope of the electrical resistivity, the optimum lamella thickness shifts to higher values for lower temperatures. In Figure 10, this is presented for 295, 77, and 4.2 K and for derivative ratios,  $k$ , of 0.8, 1, and 1.2.

$$\frac{d\tilde{P}_i}{d\tilde{P}_j} - k_{ij} = 0 \quad (2)$$

When more than one set of properties is involved, the resulting set of equations with the form of Eq. (2) cannot be satisfied simultaneously. A minimization is therefore performed, where each set of properties is given a relative weight,  $m_{ij}$ . This minimization procedure can then be applied to the function  $C(LT)$  in Eq. (3), where  $n$  is the number of properties to be combined.

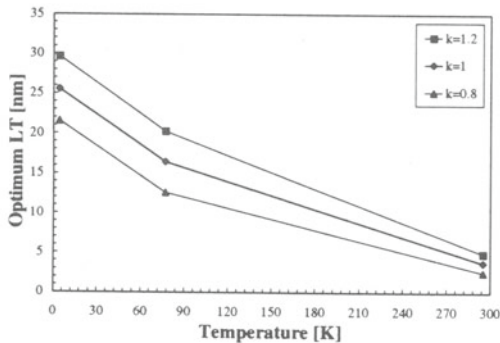
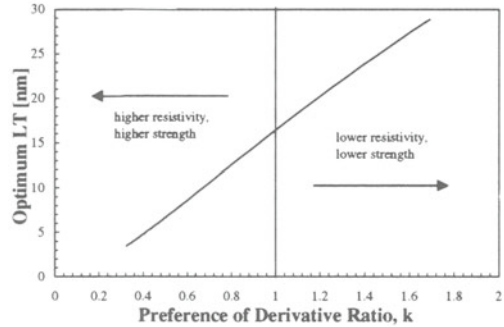
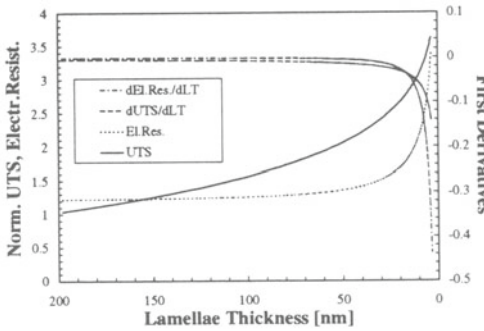


**Figure 8 (top left).** Ultimate tensile strength (UTS) and electrical resistivity at 77 K, normalized to their ROM values and their first derivatives.

**Figure 9 (top right).** Optimum lamella thickness (LT) for a combination of ultimate tensile strength and electrical resistivity at 77 K as a function of  $k$ .

**Figure 10 (left).** Optimum lamella thickness (LT) for a combination of high ultimate tensile strength and low electrical resistivity for three different  $k$  values, as a function of temperature.



Note that this formulation also applies to the case of only one combination of properties as in Eq. (2) and in fact generalizes that equation for all values of  $k_{ij}$ . In other words, while Eq. (2) can only be satisfied for a judicious choice of values  $k_{ij}$ , a minimization of Eq. (3) will always find the optimum lamella thickness for the chosen parameters.

A numeric minimization has been carried out for a combination of UTS, electrical resistivity, and thermal resistivity at 77 K (Figure 11) with  $k_{ij}=1$  for all ratios. The optimum lamella thickness of 16.5 nm for the combination of UTS and electrical resistivity only (weight factor  $m_1$ ), can be found again at  $m_2/m_1=m_3/m_1=0$ , with  $m_2$  being the weight factor for combinations of UTS and thermal resistivity and  $m_3$  for electrical and thermal resistivity. The optimum increases to 22.4 nm for  $m_2/m_1=1$  and  $m_3/m_1=0$ , to 19.2 nm for  $m_2/m_1=0$  and  $m_3/m_1=1$ , and to 23.6 nm for equal weight of all three combinations. A further increase of  $m_2/m_1=4$  or  $m_3/m_1=4$  leads to optimum values at 26.3 and 26 nm, respectively. A combination of  $m_2/m_1 = m_3/m_1=4$  leads to an optimum at 28 nm.

$$C(LT) = \sum_{\substack{i=1 \\ j>1}}^{n-1} \left[ m_{ij} * \left( \frac{d\tilde{P}_i}{d\tilde{P}_j} - k_{ij} \right)^2 \right] \quad (3)$$

## DISCUSSION

It has been confirmed by micrographic investigation that the microstructure of the as-cast state is almost entirely dominated by lamellar eutectic, as is shown in Figure 1. This is in contradiction to the theoretical expectation of rod-type eutectics for the given volume fractions, however, it may be explained by the strong non-equilibrium conditions caused by the rapid cooling. The higher internal energy of the lamellar structure, due to the higher internal interface density, may be accommodated by the energy that becomes available during the quench.

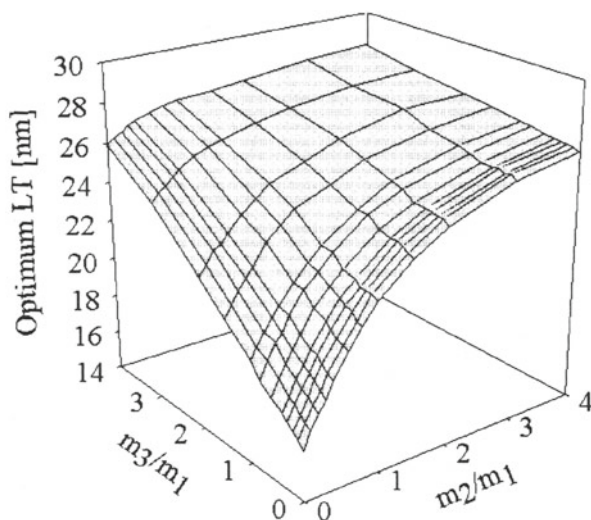


**Figure 11.** Optimum lamellae thicknesses (LT) for combinations of ultimate tensile strength, electrical resistivity, and thermal resistivity at 77 K as a function of the relative weight of their respective ratios. All  $k_{ij}$  are unity. The weight factors are  $m_1$  for a combination of UTS and electrical resistivity,  $m_2$  for UTS and thermal resistivity, and  $m_3$  for electrical resistivity and thermal resistivity.

Plastic deformation leads to a strong refinement of the average lamella thickness, as documented qualitatively in Figures 2 and 3 and quantitatively in Figures 4. The exponential reduction in lamellae thickness of both phases Ag and Cu is close to the reduction of the wire diameter (exponent =  $-0.5\eta$ ). The minor differences between Ag and Cu are in agreement with the lower flow stress of Ag but in contradiction to its lower stacking fault energy, typically leading to stronger work-hardening. Furthermore, the influence of mutual solution is not taken into consideration here. As for the quantitative description of the microstructure development for this optimization study, it was assumed that no further distinction between the Ag and Cu phases had to be made.

In order to explain the mechanical behavior of microcomposites, a variety of explanations and models have been published. Three different approaches can be found. First, the dislocation density either strongly increases, beyond what is commonly found in bulk metals, leading to very high passing stresses for mobile dislocations<sup>10</sup>, or strongly decreases, resulting in a lack of mobile dislocations<sup>8</sup>. Second, changes in morphology lead to the development of whiskers<sup>11,12</sup> or amorphous areas<sup>13,14</sup>. Third, the interaction of dislocations and internal interfaces lead to a Hall-Petch type strengthening<sup>15-17</sup>. In order to discuss the validity of each of these models for rotary-swaged Ag-Cu, high resolution TEM studies must be carried out, accounting for dislocation arrangements and densities as well as crystallographic orientation.

The variation of the resistivity with changes in microstructure can be understood in terms of the interaction of conduction electrons with the internal interfaces. Both the electrical and thermal resistivity of metals strongly depend on the mean free path of the conduction electrons. The behavior of the composite can be modeled by accounting for increased interface scattering<sup>18</sup>. With decrease in temperature, the mean free path of conduction electrons increases, leading to a greater significance of interface scattering and thus higher relative increase in resistivity.

For combinations of UTS and electrical resistivity, a distinct optimum can be found due to the different behavior of these properties with decreasing lamellae thickness. The slopes of both properties (Figure 8) are equal at only one point in the deformation process. Deformation up to this point will lead to a gain in strength that exceeds the loss in conductivity. Deformation beyond this point is accompanied by greater losses in conductivity relative to gains in strength. At 77 K, the optimum lamella thickness depends almost linearly on the derivative ratio (Figure 9), making this optimization an easy tool for determining the best microstructure for specific applications and designs.

This approach has been applied for three combinations of properties, namely UTS and electrical resistivity, UTS and thermal resistivity, and electrical resistivity and thermal resistivity. Non-trivial solutions for more than one combination of properties, i.e. more than two properties, will lead to a minimum of  $C(LT)$  greater than zero. The value of  $C_{\min}$  can be viewed as quantifying the inherent contradictions in the desired properties. Greater weight on additional property combinations that are strongly different in their behavior, e.g. UTS and thermal resistivity ( $m_2/m_1$  in Figure 11) leads to a stronger increase of the optimum lamella thickness compared to combinations of similar properties, e.g. electrical resistivity and thermal resistivity ( $m_3/m_1$  in Figure 11).

The optimization described here may be applied to any number of combinations of  $n$  properties, that have been investigated experimentally and can be expressed as a function of the lamellae thickness. Design preferences or application-dependent restrictions can be accounted for through the selection of appropriate values of  $k_{ij}$  and  $m_{ij}$ .



## SUMMARY

An approach to determine the optimum microstructure for a combination of three properties (ultimate tensile strength, electrical resistivity, and thermal resistivity) has been described and applied for eutectic Ag-Cu. The model is based on the quantitative correlation of microstructure and properties. It has been extended to account for combinations of multiple properties and incorporation of application-dependent preferences.

## ACKNOWLEDGEMENT

This work is partly based upon research conducted at the National High Magnetic Field Laboratory (NHMFL), which is supported by the National Science Foundation, under Award No. DMR-9527035.

## REFERENCES

1. J. Bevk, J. P. Harbison, and J. L. Bell, Anomalous Increase in Strength of *In Situ* Formed Cu-Nb Multifilamentary Composites, *J. of Appl. Phys.* 49(12), 6031-6038, (1978).
2. S. Foner and E. Bobrov, 68.4T Pulsed Magnet Fabricated with a Wire-Wound Metal-Matrix Cu/Nb Microcomposite, *IEEE Magnetics* 24(2), 1059-1062, (1987).
3. Y. Sakai, K. Inoue, T. Asano, and H. Maeda, Development of a High Strength, High Conductivity Copper-Silver Alloy for Pulsed Magnets, *IEEE Magnetics* 28(1), 888-891, (1992).
4. T. Asano, Y. Sakai, K. Inoue, M. Oshikiri, and H. Maeda, High-Field Pulsed Magnet Wound of Cu-Ag Alloy Wire, *J. of Appl. Phys.* 32, 1027-1029, (1993).
5. J. L. Murray, Calculation of Stable and Metastable Equilibrium Diagrams of the Ag-Cu and Cd-Zn Systems, *Metallurgical Transactions A* 15A, 261-268, (1984).
6. Y. Sakai and H.-J. Schneider-Muntau, Ultra High Strength, High Conductivity Cu-Ag Alloy Wires, *Acta Metallurgica* 45(3), 1017-1023, (1996).
7. H. E. Cline and D. Lee, Strengthening of Lamellar vs. Equiaxed Ag-Cu Eutectic, *Acta Metallurgica* 18, 315-323, (1970).
8. G. Frommeyer and G. Wassermann, Microstructure and Anomalous Mechanical Properties of *In Situ*-Produced Silver-Copper Composite Wires, *Acta Metallurgica* 23, 1353-1360, (1975).
9. K. Y. Sohn, Dissertation, University of Florida, Materials Science and Engineering, (1997).
10. P. D. Funkenbusch and T. H. Courtney, On the Strength of Heavily Cold Worked *In Situ* Composites, *Acta Metallurgica* 33(5), 913-922, (1985).
11. C. L. H. Thieme, S. Pourrahimi, and S. Foner, High-Strength Al Metal-Matrix Microcomposite Wire with 20 Vol.% Nb and Ultimate Tensile Strengths up to 1030 MPa, *Scripta Metallurgica* 28(8), 913-918, (1993).
12. F. Dupouy, Dissertation, L'Institut National Des Sciences Appliquees de Toulouse, (1995).
13. D. Kuhlmann-Wilsdorf and M. S. Bednar, Mechanisms of Metal Amorphization Through Plastic Deformation, *Scripta Metallurgica* 28(3), 371-376, (1993).
14. D. Raabe and U. Hangen, Observation of Amorphous Areas in a Heavily Cold Rolled Cu-20wt%Nb Composite, *Materials Letters* 22, 155-161, (1995).
15. W. A. Spitzig, A. R. Pelton, and F. C. Laabs, Characterization of the Strength and Microstructure of Heavily Cold Worked Cu-Nb Composites, *Acta Metallurgica* 35(10), 2427-2442, (1987).
16. U. Hangen and D. Raabe, Modeling of the Yield Strength of a Heavily Wire Drawn Cu-20%Nb Composite by Use of a Modified Linear Rule of Mixtures, *Acta Metallurgica* 43,4075-4082, (1995).
17. J. T. Wood, Dissertation, McMaster University, (1994).
18. F. Heringhaus, R. Leffers, G. Gottstein, and H.-J. Schneider-Muntau, Quantitative Correlation of Microstructure and Electrical Conductivity of a Heavily Deformed Eutectic Ag-Cu Composite in *Processing, Properties, and Applications of Cast Metal Matrix Composites* 1, edited by P. K. Rohatgi (TMS Fall Meeting), 127-142, (1996).